ELSEVIER

Physica C 299 (1998) 240–248

PHYSICA C

Effect of annealing upon the high-T_c superconductor $Bi_2Sr_2CaCu_2O_{8+\delta}$

S.T. Johnson [a,*], P.D. Hatton [b], A.J.S. Chowdhury [c], J. Gardner [d], G. Balakrishnan [d], D.McK. Paul [d], J. Hodby [c]

[a] *Department of Physics and Astronomy, University of Edinburgh, Edinburgh EH9 3JZ, Scotland, UK*
[b] *Department of Physics, University of Durham, South Road, Durham DH1 3LE, UK*
[c] *Department of Physics, University of Oxford, Clarendon Laboratory, Oxford OX1 3PU, UK*
[d] *Department of Physics, University of Warwick, Coventry CV4 7AL, UK*

Received 18 September 1997; accepted 13 November 1997

Abstract

The relationship between carrier concentration, structure and composition in $Bi_2Sr_2CaCu_2O_{8+\delta}$ is amongst the most complex of the high-T_c superconducting cuprates. In this paper a number of structural subtleties of the system are discussed based on the results of high-resolution X-ray scattering measurements from single crystals. It is found that the annealing of an oxygen-rich crystal significantly changes the character of certain diffuse scattering features. Accompanying analysis of composition and measurements of T_c suggest these changes may be the signature of oxygen ordering which is influential to the superconductivity. © 1998 Elsevier Science B.V.

Keywords: X-ray diffraction; Structure of $Bi_2Sr_2CaCu_2O_\delta$; Modulated structures; Oxygen vacancies; Structural phase transformation

1. Introduction

Control of the carrier concentration, n_h, in the CuO_2 layers of the high-T_c cuprates by variation of cation or oxygen stoichiometry in the intervening 'charge reservoir' layers has been established to be of key importance to the physical properties of these systems. It is believed [1] that the optimum value of n_h which pushes the transition temperature to its maximum for a system, T_c^{max}, is a universal parameter related only to the number of CuO_2 layers, irrespective of the chemical make-up of the intervening layers. Variations exist, however, in the value of T_c^{max} amongst systems with the same number of CuO_2 layers (the extreme example being T_c^{max} over 80 K in Tl-2201 compared with under 30 K in Bi-2201 [2]). In addition to varying n_h, cation and oxygen changes must therefore facilitate structural adjustments which hold their own more subtle influence over superconductivity. Establishing the separate effects of structure has proved difficult and remains an important challenge to full understanding of superconductivity in the cuprates.

With regard to this question, the most well stud-

* Corresponding author. Present address: Laboratoire de Physique des Solides, Bâtiment 510, Université Paris-Sud, 91405 Orsay, France. Tel: +33 1 69 155306; Fax: +33 1 69 155654; E-mail: stuart@lps.u-psud.fr.

PII S0921-4534(97)01849-2

ied system has been $YBa_2Cu_3O_{6+\delta}$ (Y-123), in which a well defined cation stoichiometry allows the T_c–n_h-structure relationship to be explored through the variation of oxygen stoichiometry δ. A remarkable level of understanding has been achieved, emphasizing the importance of oxygen ordering [3] in the CuO chain layers (the charge reservoir) in favourably influencing n_h and T_c. A complimentary system is $La_{2-x}Sr_xCuO_4$ (La-214) in which oxygen stoichiometry can be reliably fixed, and the relationship explored through cation substitutions. The results have emphasized the effect of structural distortion of the CuO_2 planes, and it has been argued that the optimum structural setting for maximizing T_c are square and flat CuO_2 planes [4].

Amongst the more complex systems, both cation and oxygen variations exist over wide and imprecisely defined ranges, involving several mixed cation sites. The departures from the crystallographic ideal which accompany these compositional variations have, in the most part, still to be confidently characterized. These comments are especially true of Bi-2212 in which the complexity is such that even the ideal crystallographic structure is not unequivocably refinable due to the existence of a displacive modulation with a period which is incommensurate with its lattice. Many studies have been undertaken, and most agree upon the form of the cation modulations [5–9] which are described by a wavevector $\boldsymbol{q} = \beta \boldsymbol{b}^* + \boldsymbol{c}^*$ with $\beta \approx 0.21$. A consensus has also emerged that areas of expansion produced by the modulation in the BiO layers facilitates the accommodation of extra oxygen [10,5], which when fully occupied increases oxygen stoichiometry from 8.0 to 8.2. However, a closer assessment of the many structural refinements [11] reveals the structure may be substantially more complicated than is assumed in this single extra-oxygen model, allowing for a considerable range in oxygen variation (from [9] $\delta = 0.0$, [7] $\delta = 0.4$, to [5] $\delta = 1.0$) and involving several additional sites. Furthermore, experiments which have explicitly measured the variation in oxygen stoichiometry due to annealing suggest that a range of variation in oxygen of $\Delta\delta > 0.2$ may be possible [12–15]. All of this suggests that the currently accepted assumptions are at best naive, and that the true degree of subtlety in the oxygen-structure relationship has yet to be discerned.

The failure to describe other structures as correctly as Y-123 is an important problem. It has been pointed out [16] that the many experiments linking subtle structural changes to the superconducting mechanism in the vicinity of T_c cannot be interpreted conclusively because of this lack of understanding. Also, important questions remain about flux-pinning mechanisms in the Bi-systems [17,18]. The results presented in this paper describe changes in diffuse X-ray scattering which may be associated with changes in oxygen content or ordering. Although neutron scattering is more suitable for this purpose, the ability to observe oxygen changes with X-rays has been well demonstrated in Y-123 [19]. The paper starts by characterizing in higher resolution than before the reciprocal space features peculiar to Bi-2212.

2. Experimental details

Of the five samples used in this work, one was flux grown using a platinum crucible (to be identified as C), two (identified as A1 and A2) were grown by the travelling solvent floating zone method (TSFZ) with a starting composition of Bi:Sr:Ca:Cu = 2:2:1:2, two others were also TSFZ grown but from a batch with a starting composition of Bi:Sr:Ca:Cu = 2.2:1.64:1.16:2.0 (identified as B1 and B2). It is known [20] that as-grown crystals from the 2212 starting mix are close to optimum doping, while the off-stoichiometric composition are overdoped and with a lower T_c. The A1 and A2 samples had dimensions $6 \times 3 \times 0.1$ mm while the B1 and B2 samples were ≈ 1–2 mm longer. The A2, B2 and C crystals were subjected to electron probe microanalysis (EPMA) to determine differences in composition.

The A1 and B1 samples underwent annealing treatments, designed to bring about an opposite effect upon T_c in each case. A1 was annealed for 24 h in an oxygen atmosphere at 720°C to lower T_c. B1 was annealed in a nitrogen atmosphere at 720°C for only 10 min (it is known from experience to be sufficient) to increase T_c. The superconducting transitions were characterized for all five crystals in their as-grown state, as well as post-anneal for A1 and B1, using AC susceptibility with H_{AC} parallel to the

c-axis. The critical temperature T_c was defined as the onset of diamagnetism.

The X-ray measurements were performed on a two-circle, triple-crystal diffractometer using a GX21 high-brilliance rotating-anode source operating at 3 kW with Cu Kα radiation. Samples were aligned on the diffractometer in Bragg reflection geometry with the reciprocal $\boldsymbol{b}^*-\boldsymbol{c}^*$ axes in the horizontal scattering plane. The triple-crystal arrangement ensures an instrumental resolution limited only by the mosaic of the crystals chosen for monochromator and analyser [21], and also provides for a well-defined resolution in two dimensions in the scattering plane. Low resolution measurements were made using pyrolytic graphite crystals which have a mosaic width of $\approx 0.4°$. High-resolution measurements utilized the (111) reflection from germanium crystals with a mosaic width of 4.3×10^{-3} degrees, the intensity is reduced by a factor of ≈ 100 but provides a resolution sufficient for measuring the intrinsic mosaic widths of any high-T_c crystal.

3. High resolution study of structural characteristics

Earlier low-resolution measurements of Bi-2212 [22,23] established the nature of the diffuse features which can be observed, with certain features identified as sample dependent. One feature, however, was observed consistently: diffuse streaks lying between satellites along the $\langle 001 \rangle$ direction. Their origin is, even now, not known, yet they appear as characteristic as the much discussed main satellites themselves. Fig. 1 illustrates the arrangement of satellites and diffuse streaks around a fundamental Bragg reflection, the measurements are from the C crystal but are typical of all the crystals studied. The streaks are visibly broadened along the $\boldsymbol{c}^*$-direction in such a way as to almost link neighbouring satellites.

The intensity distribution of the streaks relative to that of the satellites was surveyed over a large area of reciprocal space. Certain points are noteworthy. Around the (0 0 24), shown in Fig. 1a, which is a relatively weak reflection but which is surrounded by comparatively strong satellites, the diffuse streaks are entirely absent. In contrast, around the (0 0 30) in Fig. 1b, where the satellites are weak, the diffuse

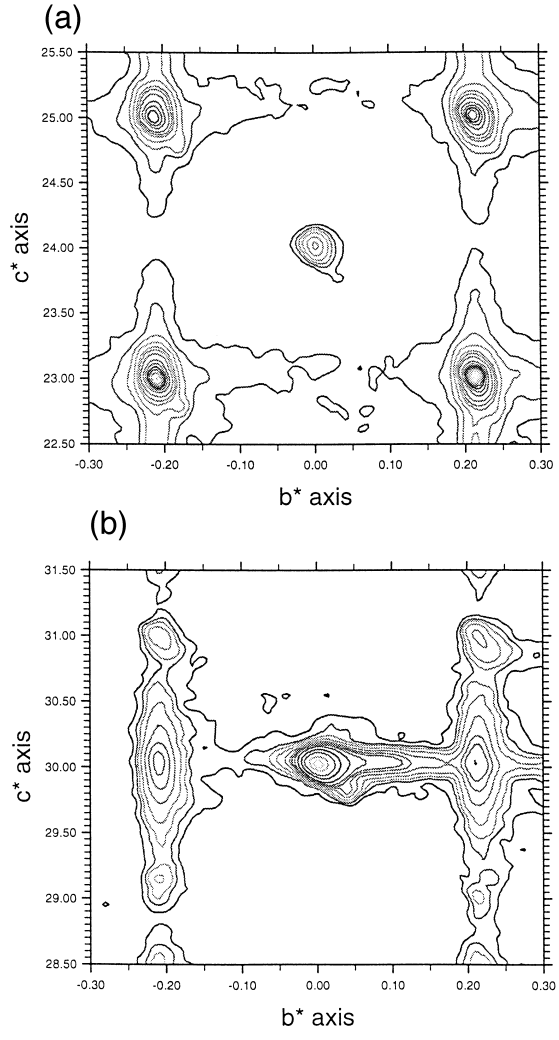

Fig. 1. Two contrasting pictures of areas of reciprocal space around different fundamental reflections; (a) the (0 0 24) and (b) the (0 0 30). The contour lines are drawn to follow an essentially logarithmic intensity scale spanning up to five orders of magnitude between the lowest background levels (typically 1–10 counts/s) and the strong fundamental reflections.

streak is more intense. The intensities of the streaks are overall closely dependent upon their fundamental reflection of origin, and this dependence is of a different nature from that of the satellite reflections.

To resolve the intrinsic widths and make a more quantitative assessment, the C and A1 crystals were studied in high-resolution mode. Fig. 2 shows the improvement between low- and high-resolution in the profile of a fundamental reflection. The widths in

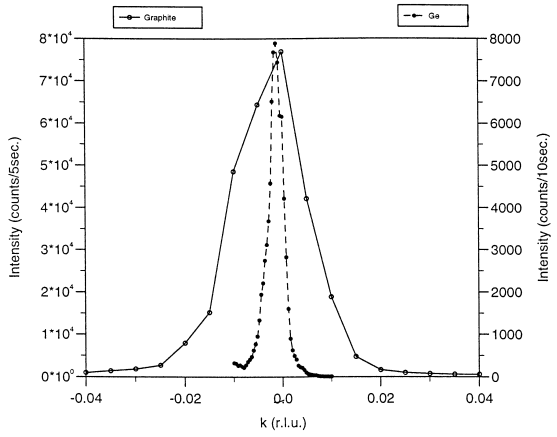

Fig. 2. Comparisons between low- and high-resolution profiles of the (0 0 20) reflection from the C crystal.

the ⟨010⟩ direction and the positions of the satellites were measured for the two crystals. The overall results are presented in Table 1 (the values are averaged from measurements of a number of reflections around the (0 0 20)). For the C crystal, the FWHM of the satellites are ≈1.5 times greater than that of the fundamental reflections, while the diffuse streaks are a further 2.5 times greater than the satellites. The FWHM values of the A1 crystal are greater but with similar proportions.

The asymmetry about the $\boldsymbol{c}^*$-axis was another feature characterized in the earlier work [22]. Shown in Fig. 3, an ill-defined profile shape is resolved by the higher resolution into two quite distinct peaks. The strongest is located at the commensurate l position, as expected. The second, weaker peak is well separated and positioned with an incommensurate value of l. Similar observations of the splitting could be made around all the satellites studied, but both the value of l and the intensity ratios varied considerably. This could be explained by domains distinguished by a variety of $\gamma\boldsymbol{c}^*$ values. The range extends as a tail from the primary satellite as far as a cut-off, which is the same in all cases, at $(1-\gamma) \approx 0.15$. In Fig. 3 two definite values are measurable, $(1-\gamma)=0.14$, and a very much weaker reflection at the intermediate value of $(1-\gamma)=0.07$. Although observable in many crystals, it is not universally so. There is a complete absence of any splitting in crystal A1 for instance. The origin of these features lies in a slight monoclinic distortion which has been refined in a study of a crystal with a single domain of the γ value [24]. The fact that both the crystals here are high quality with close to optimum values of T_c, suggests it is not significant for transport properties.

Table 1
The FWHM values and the incommensurate period measured using the high-resolution mode

	A1	C
Fundamental	0.010(1)	0.003(1)
Satellite	0.014(2)	0.005(1)
$\beta\boldsymbol{b}^*$	0.209(1)	0.209(1)
Streak	0.017(2)	0.015(2)

All values are in r.l.u.

4. Susceptibility and EPMA characterization

The results of the compositional analyses are presented in Table 2. Relative to the idealized 2212 stoichiometry A2 comes closest, while both B2 and C have increased Bi and reduced Sr contents. The oxygen values so determined give a reliable indication of the relative differences between the samples but the absolute values must be read with caution (accurate at best to 5–10%). The excess Bi of B2 combined with growth in a flowing oxygen atmosphere has resulted in a significantly increased δ relative to C and A2. The higher δ correlates with

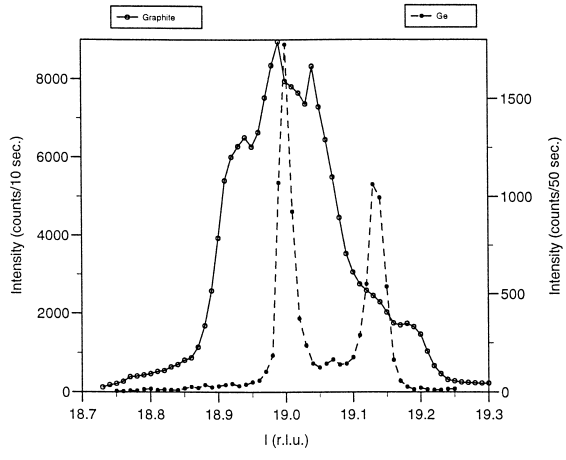

Fig. 3. $\boldsymbol{c}^*$ profiles from the C crystal of the (0 −0.21 19) satellite. The apparent splitting observed in low-resolution has been separated into distinct reflections by the higher resolution.

Table 2
The results of EPMA determination of the normalized cation stoichiometry and oxygen content of the three crystals

	Starting composition	Measured composition Bi:Sr:Ca:Cu	Oxygen δ	T_c
A2	2.0:2.0:1.0:2.0	1.970:1.810:0.915:2.00	0.013	94 K
B2	2.2:1.64:1.16:2.0	2.057:1.603:1.09:2.00	0.104	82 K
C	2.3:2.1:1.0:2.05	2.05:1.92:0.85:2.00	0.06	93 K

The starting composition is that of the initial flux.
T_c was determined by AC susceptibility.

the considerably lower T_c of 82 K, while $T_c = 94$ K for A2 and $T_c = 93$ K for C. The differences of $\Delta\delta = 0.09$ for a $\Delta T_c = 10$ K are in good agreement with those in the literature [13–15,25].

In their as-grown states, A1 and B1 show transitions similar to those of their respective partners A2 and B2. So, it can be reasonably assumed that they also share (before annealing) closely similar compositions. The A1 crystal was annealed in O_2, T_c was initially 93 K reducing to 88 K after annealing. In the case of B1, its nitrogen annealing had the reverse effect raising the as-grown T_c of 82 K to close to 86 K post-anneal. The transition widths remained essentially unaffected by the annealing in the case of A1, with some degradation in B1. The low temperature diamagnetic signal showed a marked change in both cases. The value of the remaining diamagnetism at temperatures well below the transition is an indication of the superconducting volume fraction of a sample. The observed decrease could be attributable to surface decomposition of the samples which is commonly observed to accompany exposures to temperatures above 500°C [26].

5. Annealing induced changes

The values of the lattice parameters, b and c, and of the incommensurate wavevector β were determined from the X-ray measurements, and are summarized in Table 3, for both as-grown and annealed samples. The constancy of β is notable, despite the annealing treatments and the differences in δ in the

Table 3
Lattice parameters of as-grown and annealed crystals

	b_0 (Å)	c_0 (Å)	βb^* (r.l.u.)
A1 (as-grown)	5.40(1)	30.864(5)	0.212(2)
A1 (O_2 anneal)	5.40(1)	30.854(5)	0.212(2)
B1 (as-grown)	5.37(1)	30.686(5)	0.210(2)
B1 (N_2 anneal)	5.40(1)	30.770(5)	0.212(2)
C	5.40(1)	30.910(5)	0.207(2)

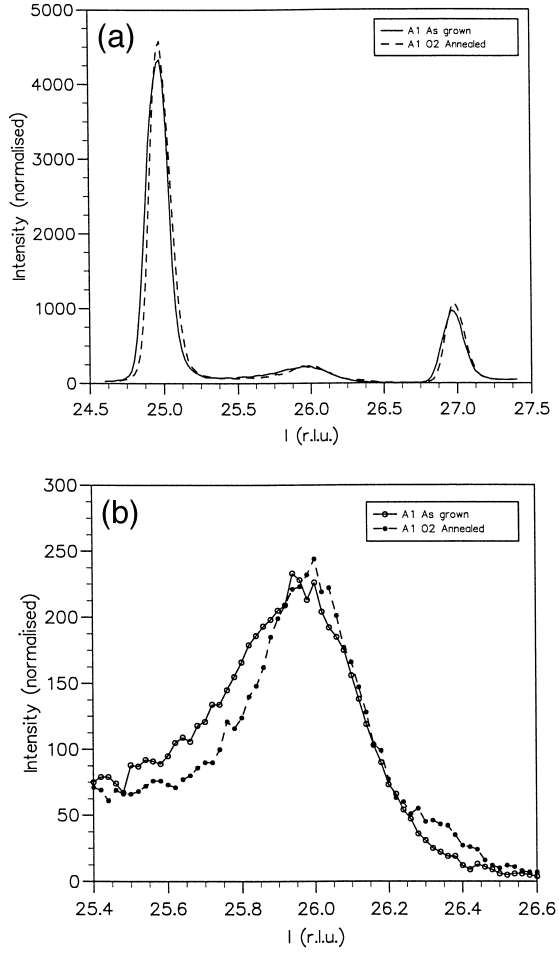

Fig. 4. Scans along (0 −0.21 it l) measured for A1 before and after annealing in oxygen; an expanded view of the diffuse streak at (0 −0.21 26) is shown in (b). Intensity values are normalized to the (0 0 26) fundamental reflection.

as-grown state. This demonstrates the value of the incommensurate wavevector cannot be considered a continuous function of oxygen, in agreement with conclusions from in situ annealing measurements [27]. The lattice parameters of B1 showed a clear change after the annealing. The ***c***-axis expanded by 0.08 Å, a change commonly reported [25,28,29] to accompany an increase in T_c.

Scans of A1 are presented in Fig. 4, in the ⟨001⟩ direction across two first-order satellites and the diffuse streak between them. There is remarkably little difference between the as-grown and annealed. Measurements of the same reflections for B1 in Fig. 5, in contrast, a pronounced change. The flattened as-grown shape of the streak has transformed after annealing into a well defined peak. This is further illustrated in Fig. 6 by the even more dramatic re-shaping of the streak at (0 −0.21 20). The increased prominence of the streaks is accompanied by a decreasing ⟨001⟩ FWHM, and decreases in the satellite intensities. The observations are indicative of a disorder-order related change having taken place. No variation in the ⟨010⟩ widths could be observed due to the limiting graphite resolution.

The intensity of the satellites relates potentially valuable information regarding the amplitude of the

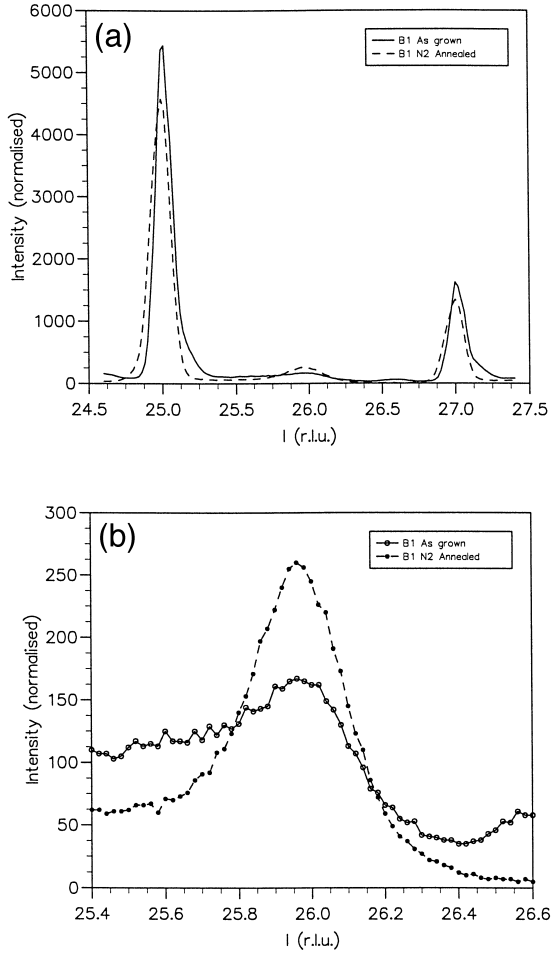

Fig. 5. Scans along (0 −0.21 it l) measured for B1 before and after annealing in nitrogen; an expanded view of the diffuse streak at (0 −0.21 26) is shown in (b). Intensity values are normalized to the (0 0 26) fundamental reflection.

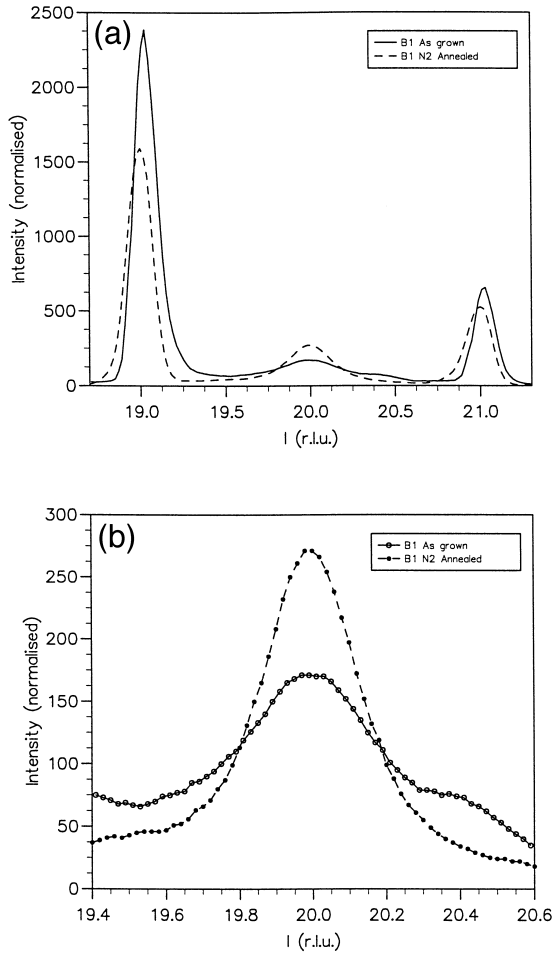

Fig. 6. Further scans for B1 before and after annealing in nitrogen, here showing the changes in the (0 −0.21 20) streak. Intensity values are normalized to the (0 0 20) fundamental reflection.

Table 4
Normalized peak intensities (±5% error) for A1 and B1 measured before and after annealing in oxygen, and nitrogen respectively

	As-grown	Annealed	Change (%)
A1			
(0 −0.21 27)	0.112	0.115	+3
(0 −0.21 25)	0.461	0.451	−2
(0 −0.21 26)^{streak}	0.022	0.020	−9
B1			
(0 −0.21 27)	0.159	0.139	−12
(0 −0.21 25)	0.555	0.460	−17
(0 −0.21 26)^{streak}	0.009	0.024	+170

modulated atomic displacements [30], and intensity changes are prominent in Figs. 4–6. The measurements have to be first normalized before comparisons can be made; the results here have all been normalized to the intensity of their parent fundamental reflection. However, there exist differences in the intensity ratios of fundamental reflections between crystals, and this makes anything other than a qualitative assessment of the manner of the changes unreliable. Measurements were made of the peak intensities from ⟨010⟩ direction scans (preferable to the ⟨001⟩ scans because they allow subtraction of the background). The data presented in Table 4 summarises the differences in normalized intensity for both satellites and streaks. B1 shows large, definite decreases in the satellites, in addition to the already discussed increase of the diffuse streaks. This indicates a decrease in the modulation's amplitude has accompanied the ordering. The changes for A1 are of an opposite sense, and of a much smaller magnitude.

6. Discussion

That the streaks are positioned with the characteristic $0.21\boldsymbol{b}^*$ value undoubtedly relates them to the modulation, and the nature of the streaking along ⟨001⟩ suggests an origin linked to interlayer disorder. However, straightforward disordering of the modulation would only broaden the satellites. Without the $\boldsymbol{c}^*$ component of $\boldsymbol{q}$, the streaks correspond to a violation of the body centred symmetry of the modulated structure. A modulation similarly lacking a $\boldsymbol{c}^*$ component is known in Pb doped Bi-systems [31,32]. The nature of the streaks, then, indicates them to be associated with a structural feature closely linked to the modulation within the basal ***ab***-plane and which disrupts its body centred symmetry, but which is poorly correlated between layers; the widths in the ⟨001⟩ direction suggest a coherence of only 2 to 3 unit cells.

The transformation of the streaks in B1 indicates that annealing brought about an ordering of this structural feature along the ***c***-axis. The annealing of A1, however, had little or no influence. The compositional analysis identified the differences between them to be the low Sr, and slightly Bi rich stoichiometry of the B samples, and a larger δ. An ordering of some cation substitutions which are not present in A1, or of the additional oxygen could therefore be explanations. A notable observation, however, is that although C has a similar Bi stoichiometry to B1, it has a diffuse streak closer instead to that of A1 in intensity and shape; both A1 and C have similar values of δ and T_c. This suggests the δ of B1 maybe the more significant parameter.

In as-grown crystals a large excess of oxygen will most reasonably be incorporated in a disordered manner, evidenced by STM images of oxygen rich Bi-2212 [33]. If oxygen is indeed at the root of the streaks, the lack of coherence in the oxygen arrangement would explain their extremely flattened shape in B1 before annealing. Refinements have suggested a number of additional oxygen sites, to little consensus, but all within the Bi_2O_2 slabs. The points of greatest separation between neighbouring BiO layers could be favourable sites, in addition to the 'bridging oxygens' identified by Le Page [34]. These positions also violate the modulation's symmetry. The subsequent ordering may be dependent upon the extent to which δ changes. The brief 10 minute anneal is, on the basis of published studies [25,35], too short a time to effect the bulk oxygen content, particularly considering the sample's dimensions. The effect may instead be to facilitate a more ordered oxygen distribution, allowing migration to energetically favoured sites. The behaviour of A1 in this picture is understandable because A1 starts with a far lower δ, and even after annealing T_c indicates δ remains lower than B1.

The reduction in satellite intensity observed to accompany the ordering is significant. Variation in

amplitude of the cation modulation is a reasonable adjustment to associate with changes in oxygen configuration because the period of the modulation is pinned [27]. A qualitative trend suggested by the data is where T_c has increased in B1 it has been accompanied by a decrease in the amplitude of the distorting modulation. The tilt of the CuO_5 octahedra is an important quantity in determining superconducting properties [36], and this would certainly alter along with the modulation's amplitude. Decreasing amplitude will also flatten the corrugation of the CuO_2 layers and this may also be influential [4]. If there was indeed little change in δ in B1, the suggested ordering could explain the increase in T_c of around 3 K by these means. The ordering may also influence interlayer coupling, and could explain the relief of interlayer distortion previously suggested by Yoo [37] to explain the change in ρ_c due to annealing.

The suggestion that structural change induced by annealing is responsible for influencing T_c has been made by other experiments when it was believed that no suitable change in δ to effect n_h could have occurred [29,38]. The most persuasive result is that obtained by Wu [39] who found that the T_c of single crystals could be raised to around 86 K by annealing but that the change was independent of both the period of anneal and, most striking, the atmosphere. It has similarly been found for samples of the B-type, that it is difficult to effect T_c beyond the initial rise to 86 K, even with greatly extended periods of annealing. Evidence of a different kind comes from Mossbauer studies of Fe doped Bi-2212 [40], which are sensitive to the CuO_2 plane distortions of the modulation. They found vacuum annealing induced changes in the local distortions, in association with the rise of T_c to its maximum.

7. Conclusion

The oxygen-structure-property relationship in Bi-2212 is a complicated one, and there remain important questions. Diffuse streaks, associated with, but distinct from satellite reflections, are a generic feature of the reciprocal space pattern [22]. The results have revealed new information about the nature of these streaks and, most importantly, observed a dramatic transformation in shape and intensity of the streaks of an oxygen rich crystal by briefly annealing. The change in shape is indicative of an ordering transition. An accompanying reduction in the amplitude of the modulation was also observed. These structural changes appear to correlate with an increase in T_c. The observations are evidence to reason that oxygen ordering maybe the root cause of the streaks. Further studies involving techniques more sensitive to oxygen ordering, such as neutron diffraction, would be required to establish the precise crystallographic sites involved.

Acknowledgements

We are grateful to H. Vass for his technical assistance in this experiment. Financial support was provided by the Engineering and Physical Sciences Research Council. STJ is grateful to the Department of Social Security for support during the writing of this paper, and to the School of Physics, The University of Birmingham for hosting its completion.

References

[1] H. Zhang, H. Sato, Phys. Rev. Lett. 70 (1993) 1697.
[2] C.C. Torardi, M.A. Subramanian, J.C. Calabrese, J. Gopalakrishnan, E.M. McCarron, K.J. Morissey, T.R. Askew, R.B. Flippen, U. Chowdhry, A.W. Sleight, Phys. Rev. B 38 (1988) 225.
[3] D. Hohlwein, in: E. Kaldis (Ed.), Materials and Crystallographic Aspects of High-T_c Superconductors, Kluwer, Dordrecht, 1994, p. 65.
[4] B. Dabrowski, Z. Wang, K. Rogacki, J.D. Jorgensen, R.L. Hitterman, J.L. Wagner, B.A. Hunter, P.G. Radaelli, D.G. Hinks, Phys. Rev. Lett. 76 (1996) 1348.
[5] A. Yamamoto, M. Onoda, E. Takayama, F. Izumi, Phys. Rev. B 42 (1990) 4228.
[6] Y. Gao, P. Coppens, D.E. Cox, A.R. Moodenbaugh, Acta Crystallogr. A 49 (1993) 141.
[7] A.A. Levin, Y.I. Smolin, Yu.F. Shepelev, J. Phys.-Condens. Matter 19 (1994) 3539.
[8] A.I. Beskrovnyi, M. Dlouha, Z. Jirak, S. Vratislav, Physica C 166 (1990) 79.
[9] G. Calestani, C. Rizzoli, M.G. Francesconi, G.D. Andreetti, Physica C 161 (1989) 598.
[10] G. Miehe, T. Vogt, H. Fuess, M. Wilhelm, Physica C 171 (1990) 339.
[11] S.T. Johnson, Ph.D. Thesis, The University of Edinburgh, 1995.
[12] R.G. Buckley, J.L. Tallon, I.W. Brown, M.R. Presland, N.E.

Flower, P.W. Gilberd, M. Bowden, N.B. Milestone, Physica C 156 (1988) 629.
[13] D.E. Morris, C.T. Hultgren, A.M. Markelz, J.Y.T. Wei, N.G. Asmar, J.H. Nickel, Phys. Rev. B 38 (1989) 6612.
[14] D.B. Mitzi, L.W. Lombardo, A. Kapitulnik, S.S. Laderman, R.D. Jacowitz, Phys. Rev. B 41 (1990) 6564.
[15] Th. Schweizer, R. Muller, J.J. Gauckler, Physica C 225 (1994) 143.
[16] T.R. Sendyka, W. Dmowski, T. Egami, N. Seiji, H. Yamauchi, S. Tanaka, Phys. Rev. B 51 (1995) 6747.
[17] P.H. Kes, in: E. Kaldis (Ed.), Materials and Crystallographic Aspects of High-T_c Superconductors, Kluwer, Dordrecht, 1994, p. 65.
[18] G. Yang, P. Shang, S.D. Sutton, I.P. Jones, J.S. Abell, C.E. Gough, Phys. Rev. B 48 (1993) 4054.
[19] T. Zeiske, D. Hohlwein, R. Sonntag, F. Kubanek, T. Wolf, Physica C 194 (1992) 1.
[20] G. Balakrishnan, D.McK. Paul, M.R. Lees, A.T. Boothroyd, Physica C 219 (1994) 61.
[21] C.A. Lucas, E. Gartstein, R.A. Cowley, Acta Crystallogr. A 45 (1989) 416.
[22] S.T. Johnson, P.D. Hatton, A.J.S. Chowdury, B.M. Wanklyn, Y.F. Yan, Z.X. Zhao, A. Marshall, Physica C 219 (1994) 64.
[23] C. Patterson, P.D. Hatton, R.J. Nelmes, X. Chu, Y.F. Yan, Z.X. Zhao, Superconduct. Sci. Technol. 3 (1990) 297.
[24] R.E. Gladyshevskii, R. Flukiger, Acta Crystallogr. B 52 (1996) 38.
[25] T.W. Li, P.H. Kes, W.T. Fu, A.A. Menovsky, J.J.M. Franse, Physica C 224 (1994) 110.
[26] W. Wu, F. Li, X.-G. Li, L. Shi, G. Zhou, Y. Qian, Q. Qin, Y. Zhang, J. Appl. Phys. 74 (1993) 4262.
[27] S.T. Johnson, P.D. Hatton, Physica C 270 (1996) 41.
[28] J.H.P.M. Emmen, S.K.J. Lenczowski, J.H.J. Dalderop, V.A.M. Brabers, J. Cryst. Growth 118 (1992) 477.
[29] W.A. Groen, D.M. de Leeuw, Physica C 159 (1989) 417.
[30] H.Z. Cummins, Phys. Rep. 185 (1990) 211.
[31] O. Eibl, Physica C 168 (1990) 215.
[32] L. Pierre, J. Schneck, J.C. Toledano, C. Daguet, Phys. Rev. B 41 (1990) 766.
[33] V.P.S. Awana, S.B. Samanta, P.K. Dutta, E. Gmelin, A.V. Narlikar, J. Phys.-Condens. Matter 3 (1991) 8893.
[34] Y. Le Page, W.R. McKinnon, J.M. Tarascon, P. Barboux, Phys. Rev. B 40 (1989) 6810.
[35] M. Runde, J.L. Routbort, S.J. Rothman, K.C. Goretta, J.N. Mundy, X. Xu, J.E. Baker, Phys. Rev. B 43 (1992) 7375.
[36] B. Buchner, M. Breuer, A. Freimutth, A.P. Kampf, Phys. Rev. Lett. 73 (1994) 1841.
[37] K.-H. Yoo, D.H. Ha, Y.K. Park, J.C. Park, Phys. Rev. B 49 (1994) 4399.
[38] M. Nagoshi, T. Suzuki, Y. Fukuda, K. Terashima, Y. Nakanishi, M. Ogita, A. Tokiwa, Y. Syono, M. Tachiki, Phys. Rev. B 43 (1991) 10445.
[39] W. Wu, L. Wang, Q. Qin, Y. Qian, L. Shi, X. Li, G. Zhou, Y. Zhang, Phys. Rev. B 49 (1994) 1315.
[40] S.T. Lin, W.S. Chung, C.Y. Chou, C.M. Lin, J. Phys.-Condens. Matter 2 (1990) 8673.